

# Identification of potential biomarkers and pivotal biological pathways for prostate cancer using bioinformatics analysis methods

Zihao He<sup>1,2,3</sup>, Xiaolu Duan<sup>1,2,3</sup> and Guohua Zeng<sup>1,2,3</sup>

<sup>1</sup> Department of Urology, Minimally Invasive Surgery Center, The First Affiliated Hospital of Guangzhou Medical University, Guangzhou, China

<sup>2</sup> Guangzhou Institute of Urology, Guangzhou, China

<sup>3</sup> Guangdong Key Laboratory of Urology, Guangzhou, China

## ABSTRACT

**Background:** Prostate cancer (PCa) is a common urinary malignancy, whose molecular mechanism has not been fully elucidated. We aimed to screen for key genes and biological pathways related to PCa using bioinformatics method.

**Methods:** Differentially expressed genes (DEGs) were filtered out from the [GSE103512](#) dataset and subjected to the gene ontology (GO) and Kyoto Encyclopedia of Genes and Genomes (KEGG) pathway analyses. The protein-protein interactions (PPI) network was constructed, following by the identification of hub genes. The results of former studies were compared with ours. The relative expression levels of hub genes were examined in The Cancer Genome Atlas (TCGA) and Oncomine public databases. The University of California Santa Cruz Xena online tools were used to study whether the expression of hub genes was correlated with the survival of PCa patients from TCGA cohorts.

**Results:** Totally, 252 (186 upregulated and 66 downregulated) DEGs were identified. GO analysis enriched mainly in “oxidation-reduction process” and “positive regulation of transcription from RNA polymerase II promoter”; KEGG pathway analysis enriched mostly in “metabolic pathways” and “protein digestion and absorption.”

Kallikrein-related peptidase 3, cadherin 1 (CDH1), Kallikrein-related peptidase 2 (KLK2), forkhead box A1 (FOXA1), and epithelial cell adhesion molecule (EPCAM) were identified as hub genes from the PPI network. CDH1, FOXA1, and EPCAM were validated by other relevant gene expression omnibus datasets. All hub genes were validated by both TCGA and Oncomine except KLK2. Two additional top DEGs (ABCC4 and SLPI) were found to be associated with the prognosis of PCa patients.

**Conclusions:** This study excavated the key genes and pathways in PCa, which might be biomarkers for diagnosis, prognosis, and potential therapeutic targets.

Submitted 1 July 2019

Accepted 11 September 2019

Published 4 October 2019

Corresponding author

Guohua Zeng,  
gzgyzgh@vip.tom.com

Academic editor

Imran Khan

Additional Information and  
Declarations can be found on  
page 15

DOI [10.7717/peerj.7872](https://doi.org/10.7717/peerj.7872)

© Copyright  
2019 He et al.

Distributed under  
Creative Commons CC-BY 4.0

OPEN ACCESS

**Subjects** Bioinformatics, Oncology, Data Mining and Machine Learning

**Keywords** Bioinformatics analysis, Prostate cancer, Differentially expressed genes, Biological pathways

## INTRODUCTION

According to the Cancer Statistics of 2019, prostate cancer (PCa) has emerged as the second most frequently diagnosed malignancy and is estimated to be the second leading

cause of cancer-related mortalities among American males ([Siegel, Miller & Jemal, 2019](#)). At present, prostate specific antigen (PSA) has been the most routinely used biomarker for the screening and monitoring of PCa ([Gandaglia et al., 2019](#)). However, elevated PSA does not necessarily indicate PCa and often leads to false positive results as well as overdiagnosis since it can also be seen in other benign lesions such as prostatitis or benign prostatic hyperplasia ([Inahara et al., 2006](#); [Liu et al., 2019b](#)). Therefore, excavating reliable and effective biomarkers and learning hub genes involved in the biological process (BP) of PCa is urgently needed.

With the development of high-throughput sequencing technology and bioinformatic analysis methods, the gene expression omnibus (GEO) online public database has been widely utilized to screen out differentially expressed genes (DEGs), to study molecular signals and their relations, and to aid in constructing gene regulatory networks ([Clough & Barrett, 2016](#)). Up to now, by either analysis of a single dataset or integrated analysis of multiple datasets in GEO, several studies have dug out genes that exert important influence on the occurrence and progression of PCa, such as cadherin 1 (CDH1) ([Fang et al., 2017](#)), CDCA8 ([Zhao et al., 2017](#)), RPS21 ([Fan et al., 2018](#)), PIK3R1 ([He et al., 2018](#)), epithelial cell adhesion molecule (EPCAM) ([Lu & Ding, 2019](#)), LMNB1 ([Song et al., 2019b](#)), IGF2 ([Tan, Jin & Wang, 2019](#)), and IKZF1 ([Tong, Song & Deng, 2019](#)). However, the key genes detected by the above studies are largely different from each other and had little in common, and such discrepancy could be attributed to the fact that PCa is considered as a heterogenous disease as a whole ([Liu et al., 2019a](#); [Thomas & Pachynski, 2018](#)). As a consequence, further studies in this regard is still required for the exploration and validation of key genes.

In [Brouwer-Visser et al. \(2018\)](#) studied the immune microenvironment in four solid cancer types including PCa and uploaded the corresponding gene expression profile dataset [GSE103512](#). For the first time, the present study employed the [GSE103512](#) dataset to screen out the DEGs between 60 PCa and seven matched normal prostate (NP) tissue, and a total of 252 DEGs were detected. The gene ontology (GO) functional annotation and Kyoto Encyclopedia of Genes and Genomes (KEGG) pathway enrichment analysis of the DEGs were performed, following by the construction of the protein–protein interaction (PPI) network which could uncover the underlying molecular mechanisms involved in the development of PCa. The cytoHubba and MCODE plugins of the Cytoscape software was applied to identify the hub genes and functional modules in the constructed PPI network, respectively. The Cancer Genome Atlas (TCGA) database, the Oncomine database, and the results reported by former studies were utilized for validation of our outcomes.

## MATERIALS AND METHODS

### Microarray data

The [GSE103512](#) gene expression profile CEL files, which consisted of 60 PCa samples of different TNM staging and Gleason grading and seven matched NP samples ([Brouwer-Visser et al., 2018](#)), were downloaded from the GEO database (<https://www.ncbi.nlm.nih.gov/geo/>). The gene probe IDs in the CEL files were converted to their corresponding gene symbols based on the annotation information of the platform GPL13158 (Affymetrix HT HG-U133+ PM Array Plate), which contains 54,715 probes.

## Data processing and screening of DEGs

The CEL files of [GSE103512](#) were read using the affy package of the R programming language (Ver. 3.6.0). Data preconditioning (including background adjustment, normalization, and summarization) were performed using the Robust Multi-array Average method. The limma package of R was adopted to identify the DEGs between PCa and NP samples, with a  $|\log_2 \text{fold change}| \geq 1$  and a  $P < 0.05$  was deemed to be of statistically significance ([Ritchie et al., 2015](#)). The overall upregulated and downregulated DEGs information were saved for further analyses.

## Functional and enrichment analyses of DEGs

The present study adopted the Database for Annotation Visualization and Integrated Discovery (DAVID; <https://david.ncifcrf.gov/>) to obtain GO annotation and KEGG pathway enrichment information of the DEGs identified previously ([Dennis et al., 2003](#)). Results with  $P < 0.05$  with count number  $\geq 2$  were regarded as statistically significant.

## PPI network construction and modules analyses

Protein–protein interaction analysis serves as an entry point for better interpretation of relationships between different proteins on a genome-wide scale, and might be helpful to provide novel insights into protein function explanation ([Stelzl et al., 2005](#)). PPI relationships of DEGs was analyzed and the corresponding PPI network was constructed by the Search Tool for the Retrieval of Interacting Genes (STRING) database online tool (<http://string-db.org/>) ([Von Mering et al., 2003](#)). All DEGs were subsequently submitted to the Cytoscape software for network visualization and hub gene identification, which was realized by the cytoHubba plugin. In addition, the MCODE plugin of Cytoscape was applied to identify potential functional modules in the PPI network with default parameters (degree cutoff  $\geq 2$ , node score cutoff  $\geq 2$ ,  $K$ -core  $\geq 2$ , and max depth = 100) ([Bandettini et al., 2012](#)).

## Validation of hub genes

First, we performed a literature search regarding gene expression profiles of PCa in Pubmed and then extracted hub genes reported by the eligible studies, which was used to compare with those identified in the present study. Next, we examined the relative mRNA expression levels of the identified hub genes using the Gene Expression Profiling Interactive Analysis (GEPIA) and Oncomine online tools for further validation. The GEPIA (<http://gepia.cancer-pku.cn/>) provides comprehensive online services based on TCGA database, and we used the differential expression analysis and patient survival analysis functions in this case ([Tang et al., 2017](#)). The Oncomine online database (<https://www.oncomine.org/>) was applied to examine the mRNA expression of hub genes in both multiple cancers and their corresponding normal tissues ([Rhodes et al., 2004](#)).

## Survival analysis of hub genes

Provided by the University of California Santa Cruz (UCSC), the UCSC Xena online tools (<https://xenabrowser.net>) enables researchers to study functional genomic

**Table 1** Top 10 upregulated and downregulated DEGs between PCa and NP tissues.

Gene symbol	Log <sub>2</sub> FC	adj.P.Val	State
NPY	-3.362711603	0.000789175	Upregulated
TARP	-3.206862002	4.85E-09	Upregulated
OR51E2	-2.828448822	7.28E-05	Upregulated
NKX3-1	-2.528690546	3.58E-12	Upregulated
MSMB	-2.517978536	5.11E-06	Upregulated
ACPP	-2.474802744	2.29E-09	Upregulated
SLC45A3	-2.46284327	2.66E-08	Upregulated
C15orf21	-2.327851135	0.003615423	Upregulated
ABCC4	-2.261776258	1.46E-08	Upregulated
LOC100287445	-2.170028348	0.000544702	Upregulated
FOLR1	3.005860886	8.83E-09	Downregulated
KRT13	2.958317838	2.03E-08	Downregulated
SEMG1	2.881097184	0.001633121	Downregulated
SEMG2	2.444264593	0.00246384	Downregulated
OLFM4	2.410939695	0.000494142	Downregulated
SLPI	2.391184301	3.98E-05	Downregulated
SCGB1A1	2.324648206	2.40E-05	Downregulated
OSR1	2.028908547	3.00E-15	Downregulated
HSPB6	1.791949206	1.19E-06	Downregulated
CFD	1.71042558	1.42E-09	Downregulated

**Note:**

DEG, differentially expressed gene; PCa, prostate cancer; NP, normal prostate; FC, fold change; adj.P.Val, adjusted P-value.

datasets for correlations between genomic and/or phenotypic variables. In this case we used this tool to study whether the expression of hub genes was correlated with the survival of PCa patients from TCGA cohorts. Patients were categorized into a relatively high and low expression group respectively based on the median expression value of genes, and their overall survivals (OSs) were analyzed using the Kaplan-Meier method with a log-rank test. A  $P < 0.05$  was deemed as statistically significant.

## RESULTS

### Data processing and screening of DEGs

The PCa microarray expression dataset [GSE103512](#) contained information of mRNA expression of 60 PC samples and seven matched NP samples. A total of 19,918 official gene symbols were discerned and the gene expression matrix was constructed. The DEGs were filtered using the limma R package (criteria: adjusted  $P < 0.05$  and  $|\log_2 \text{fold change}| \geq 1$ ). A total of 252 DEGs were identified between PCa and NP samples, including 186 upregulated genes and 66 downregulated genes. The top 10 upregulated and downregulated DEGs based on fold changes are listed in [Table 1](#). The volcano plot of all the genes detected and the cluster heatmap of the 252 DEGs were collected in [Fig. 1](#).

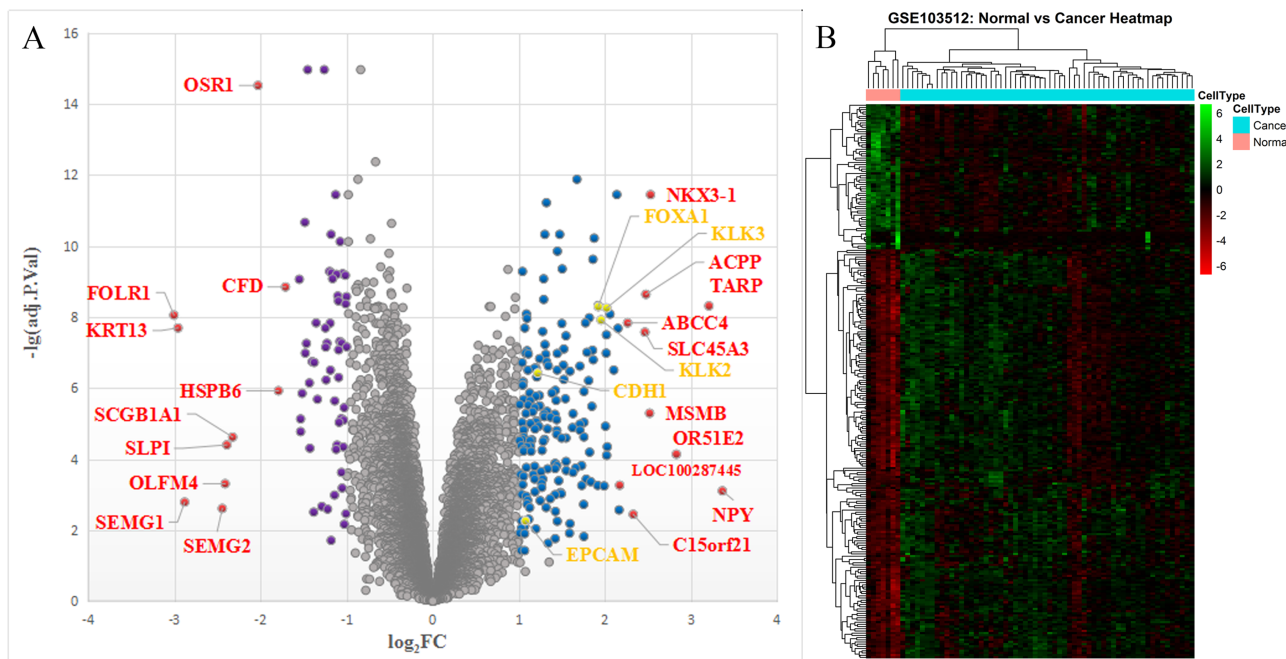


**Figure 1** The volcano plot and heatmap of the DEGs. (A) Volcano plot: The abscissa represents  $\log_2 FC$  and the ordinate represents  $-\log_{10}(\text{adjusted } P\text{-value})$ . The blue, purple, gray, red, and yellow dots represent significantly upregulated DEGs, significantly downregulated DEGs, insignificant DEGs, top 10 up/downregulated DEGs, and hub genes between PCa and NP tissues, respectively. (B) Cluster heatmap of the DEGs. DEG, differentially expressed gene; FC, fold change; PCa, prostate cancer; NP, normal prostate. Full-size DOI: [10.7717/peerj.7872/fig-1](https://doi.org/10.7717/peerj.7872/fig-1)

## Functional and pathway enrichment analyses of DEGs

Gene ontology function annotation of the identified DEGs was obtained using the DAVID database and its online analysis tool, which included the following three portions: BP, cell component (CC), and molecular function (MF). The results were deemed as statistically significant if  $P < 0.05$ , and the top 15 GO terms of the upregulated and downregulated DEGs are compiled in Table 2. As shown in Fig. 2A, the upregulated genes were mainly enriched in oxidation-reduction process (ontology: BP), extracellular exosome (ontology: CC), and calcium ion binding (ontology: MF). As shown in Fig. 2B, the downregulated genes were mainly enriched in positive regulation of transcription from RNA polymerase II promoter (ontology: BP), extracellular exosome (ontology: CC), and protein binding (ontology: MF).

The ensuing KEGG pathway analyses were also performed using the online analysis tool of DAVID database and the results were collected in Table 3. As shown in Fig. 2C, the upregulated DEGs enriched in five pathways: (1) metabolic pathways, (2) fatty acid (FA) metabolism, (3) arginine and proline metabolism, (4) Peroxisome-activated receptor (PPAR) signaling pathway, and (5) FA biosynthesis. As shown in Fig. 2D, the downregulated DEGs enriched in five pathways: (1) protein digestion and absorption, (2) aldosterone-regulated sodium reabsorption, (3) carbohydrate digestion and absorption, (4) mineral absorption, and (5) endocrine and other factor-regulated calcium reabsorption. The KEGG pathways bubble plot of all DEGs was presented in Fig. 3.

**Table 2** Top 15 enriched gene ontology terms of the upregulated and downregulated DEGs.

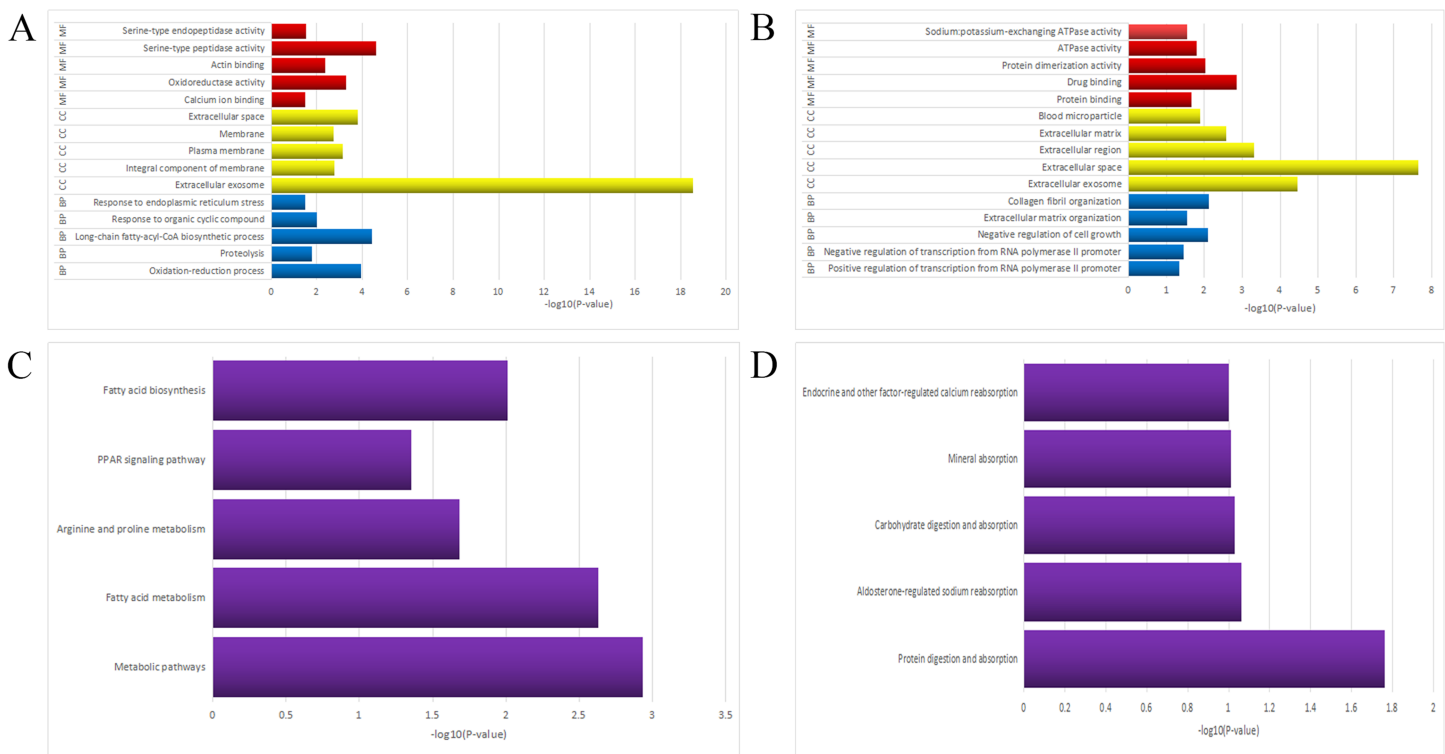
Category	Term	Count	P-value	State
BP	Oxidation-reduction process	17	1.10E-04	Upregulated
BP	Proteolysis	11	0.01703296	Upregulated
BP	Long-chain fatty-acyl-CoA biosynthetic process	6	3.93E-05	Upregulated
BP	Response to organic cyclic compound	4	0.01023923	Upregulated
BP	Response to endoplasmic reticulum stress	4	0.031611372	Upregulated
CC	Extracellular exosome	74	2.91E-19	Upregulated
CC	Integral component of membrane	65	0.001627446	Upregulated
CC	Plasma membrane	56	7.29E-04	Upregulated
CC	Membrane	34	0.00188457	Upregulated
CC	Extracellular space	27	1.58E-04	Upregulated
MF	Calcium ion binding	13	0.032748281	Upregulated
MF	Oxidoreductase activity	9	5.26E-04	Upregulated
MF	Actin binding	9	0.004195153	Upregulated
MF	Serine-type peptidase activity	7	2.40E-05	Upregulated
MF	Serine-type endopeptidase activity	7	0.030442507	Upregulated
BP	Positive regulation of transcription from RNA polymerase II promoter	8	0.047270726	Downregulated
BP	Negative regulation of transcription from RNA polymerase II promoter	7	0.034624047	Downregulated
BP	Negative regulation of cell growth	4	0.008047189	Downregulated
BP	Extracellular matrix organization	4	0.028910713	Downregulated
BP	Collagen fibril organization	3	0.007739592	Downregulated
CC	Extracellular exosome	23	3.41E-05	Downregulated
CC	Extracellular space	20	2.27E-08	Downregulated
CC	Extracellular region	15	4.96E-04	Downregulated
CC	Extracellular matrix	6	0.002673098	Downregulated
CC	Blood microparticle	4	0.013152355	Downregulated
MF	Protein binding	34	0.021626321	Downregulated
MF	Drug binding	4	0.001392245	Downregulated
MF	Protein dimerization activity	4	0.009398722	Downregulated
MF	ATPase activity	4	0.016027571	Downregulated
MF	Sodium:potassium-exchanging ATPase activity	2	0.028658029	Downregulated

**Note:**

BP, biological process; CC, cell component; MF, molecular function.

**PPI network construction and modules analyses**

The STRING online database was applied to analyze the 252 identified DEGs and to construct a PPI network, which consisted of 181 nodes interacting with each other via 403 edges. The results were downloaded for further analysis by Cytoscape software. According to the descending order of degree value, the top five hub genes were subsequently screened, namely Kallikrein-related peptidase 3 (KLK3), CDH1, Kallikrein-related peptidase 2 (KLK2), forkhead box A1 (FOXA1), and EPCAM, as presented in [Table 4](#).

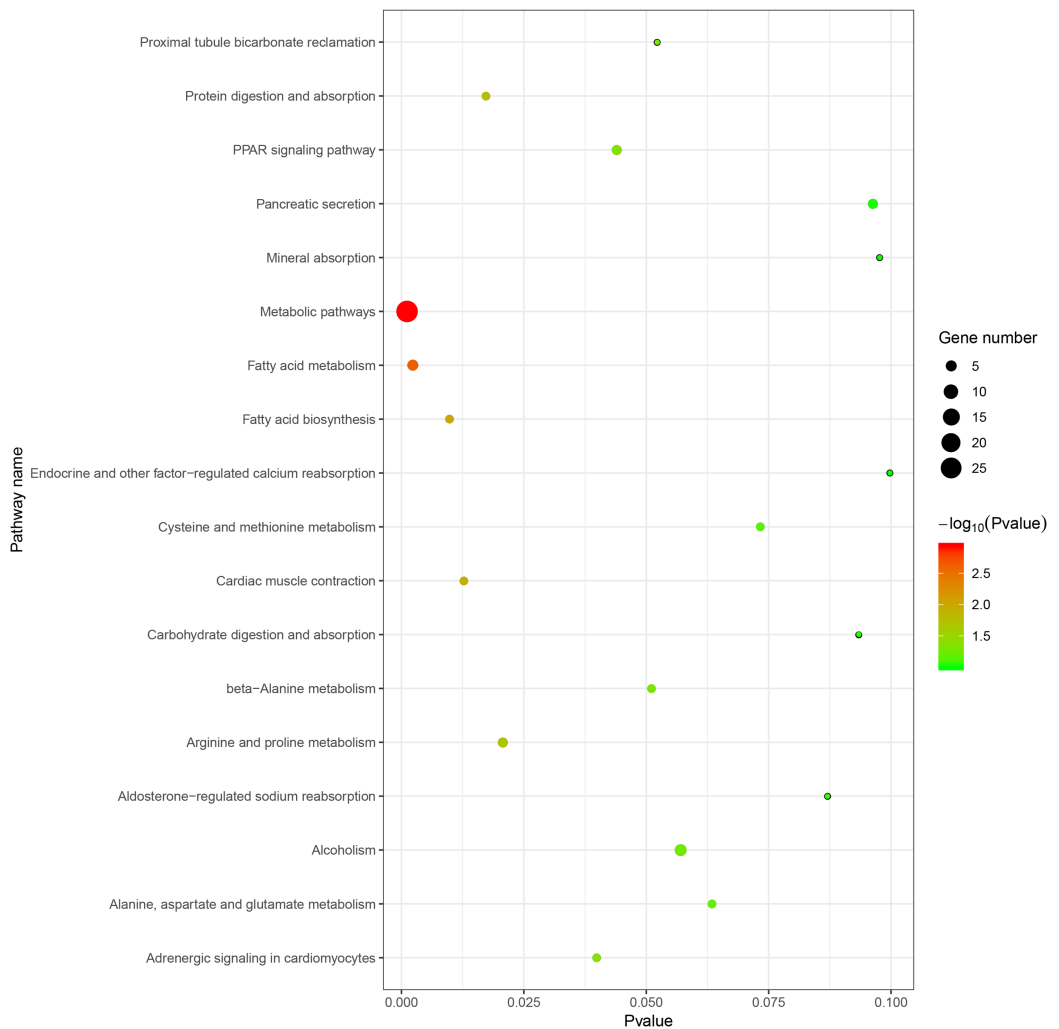


**Figure 2** The GO/KEGG enrichment analyses of the DEGs. (A) Top 15 enriched GO terms of the upregulated DEGs. (B) Top 15 enriched GO terms of the downregulated DEGs. (C) Top five enriched pathways of the upregulated DEGs. (D) Top five enriched pathways of the downregulated DEGs. GO, Gene Ontology; KEGG, Kyoto Encyclopedia of Genes and Genomes; BP, biological process; CC, cell component; MF, molecular function.

Full-size DOI: 10.7717/peerj.7872/fig-2

**Table 3** Top 5 enriched pathways of the upregulated and downregulated DEGs.

Pathway ID	Name	Count	P-value	Genes	State
hsa01100	Metabolic pathways	27	0.001161421	SAT1, NAMPT, SORD, GCNT2, GALNT7, GLUD1, PPT1, GGT1, ACSL1, ALDH1A3, ARG2, FASN, AMD1, ACSL3, DHCR24, UAP1, ACLY, ADI1, RDH11, FOLH1, ALOX15B, PLA2G7, PLA2G2A, ABAT, MBOAT2, SMS, DCXR	Upregulated
hsa01212	Fatty acid metabolism	5	0.002342524	ACSL1, SCD, FASN, PPT1, ACSL3	Upregulated
hsa00330	Arginine and proline metabolism	4	0.020729538	SAT1, ARG2, AMD1, SMS	Upregulated
hsa03320	PPAR signaling pathway	4	0.043990087	ACSL1, SCD, DBI, ACSL3	Upregulated
hsa00061	Fatty acid biosynthesis	3	0.009820063	ACSL1, FASN, ACSL3	Upregulated
hsa04974	Protein digestion and absorption	3	0.017282616	ATP1B1, ATP1A2, COL5A3	Downregulated
hsa04960	Aldosterone-regulated sodium reabsorption	2	0.087044909	ATP1B1, ATP1A2	Downregulated
hsa04973	Carbohydrate digestion and absorption	2	0.093437569	ATP1B1, ATP1A2	Downregulated
hsa04978	Mineral absorption	2	0.097676003	ATP1B1, ATP1A2	Downregulated
hsa04961	Endocrine and other factor-regulated calcium reabsorption	2	0.099788246	ATP1B1, ATP1A2	Downregulated

**Figure 3** The KEGG pathways bubble plot of DEGs.

Full-size DOI: 10.7717/peerj.7872/fig-3

**Table 4** Top five hub genes in the protein–protein interaction (PPI) network.

Gene symbol	Gene description	Degree	Log <sub>2</sub> FC	P-Value
KLK3	Kallikrein-related peptidase 3	26	2.019308668	2.04E-11
CDH1	Cadherin 1	22	1.21816524	5.18E-09
KLK2	Kallikrein-related peptidase 2	21	1.954704556	5.64E-11
FOXA1	Forkhead Box A1	20	1.922009952	1.66E-11
EPCAM	Epithelial cell adhesion molecule	19	1.076626501	0.000999371

Furthermore, seven functional cluster modules were filtered from the PPI network using the Molecular Complex Detection (MCODE) plugin of the Cytoscape software, and the top two modules (**Fig. 4**) were selected for further KEGG pathway enrichment analyses using the DAVID database. As shown in **Table 5**, the results indicated that the genes in Module 1 are mainly enriched in adherens junction and Hippo signaling pathway;

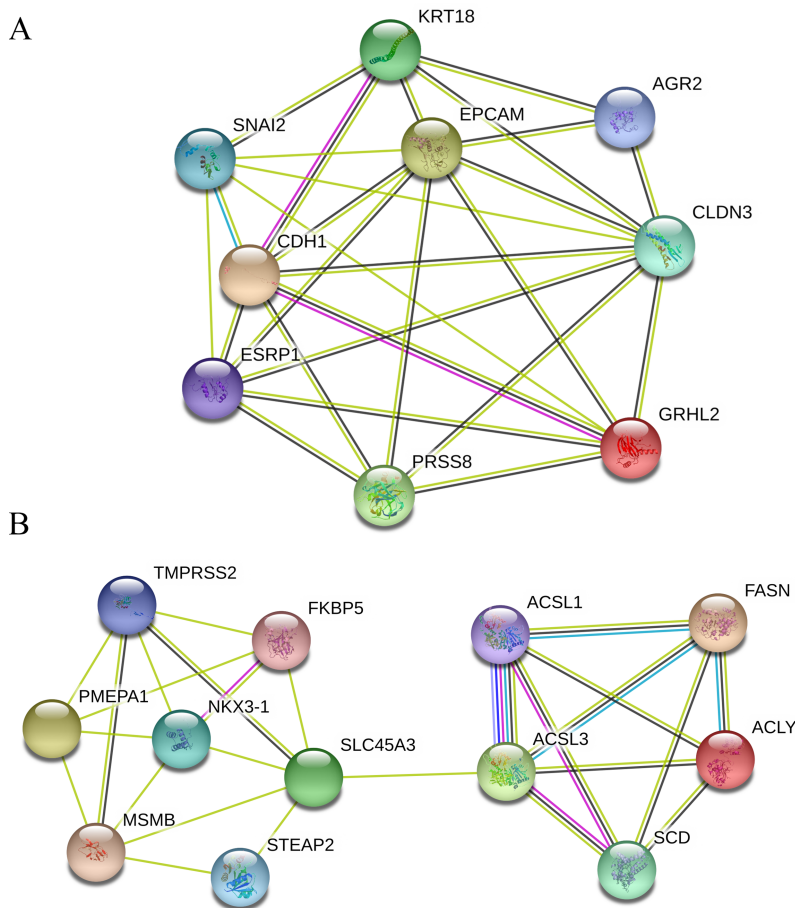


**Figure 4** Top two modules extracted from the PPI network. (A) Module 1. (B) Module 2. Circles represent genes, lines represent interactions between gene-encoded proteins and line colors represent evidence of interactions between proteins. PPI, protein–protein interaction.

Full-size DOI: 10.7717/peerj.7872/fig-4

**Table 5** Pathway enrichment analysis of the genes in the top two Modules.

Module	Pathway	Count	P-value	Genes
Module 1	Adherens junction	2	1.0E-2	CDH1, SNAI2
	Hippo signaling pathway	2	2.0E-2	CDH1, SNAI2
Module 2	Fatty acid metabolism	4	1.97E-05	ACSL1, SCD, FASN, ACSL3
	Fatty acid biosynthesis	3	9.79E-05	ACSL1, FASN, ACSL3
	PPAR signaling pathway	3	0.002925067	ACSL1, SCD, ACSL3
	Fatty acid degradation	2	0.047850686	ACSL1, ACSL3

while the genes in Module 2 are mainly enriched in FA metabolism, FA biosynthesis, PPAR signaling pathway, and FA degradation.

### Validation of hub genes expression in multiple databases

As shown in Table 6, the literature search in Pubmed/GEO regarding gene expression profiles of PCa versus NP tissues yielded 10 relevant studies, five ([Chen et al., 2012](#); [Endo](#)

**Table 6** Comparisons between the present study and other studies using the GEO datasets.

Study	Dataset	Sample size (PCa, NP)	Hub genes
<i>Endo et al. (2009)</i>	-	3, 1	TSPAN1, BMPR1B, <b>FOXA1</b> , STEAP1, RCAN3, S100P, LYZ, SCGB3A1, IL8, DPT
<i>Chen et al. (2012)</i>	-	4, 4	PPFIA2, PTPRT, PTPRR, PRR16, CHRM2, KRT23, CYP3A4, CYP3A7, DPYS, DUOXA1
<i>Fang et al. (2017)</i>	GSE26910	6, 6	<b>CDH1</b> , BMP2, NKX3-1, PPARG, PRKAR2B
<i>Zhao et al. (2017)</i>	GSE38241, GSE3933	47, 37	CDCA8, CDCA5, UBE2C, TK1
<i>Fan et al. (2018)</i>	GSE55945	18, 8	RPS21, FOXO1, BIRC5, POLR2H, RPL22L1, NPM1
<i>He et al. (2018)</i>	GSE46602	36, 14	PIK3R1, BIRC5, ITGB4, RRM2, TOP2A, ANXA1, LPAR1, ITGB8
<i>Lu &amp; Ding (2019)</i>	GSE32448, GSE45016, GSE46602, GSE104749	90, 59	<b>EPCAM</b> , TWIST1, CD38, VEGFA
<i>Song et al. (2019b)</i>	GSE6919, GSE6956, GSE32448, GSE32571, GSE35988, GSE46602, GSE68555, GSE69223, GSE70768, GSE88808	569, 402	LMNB1, TK1, RACGAP1, ZWINT
<i>Tan, Jin &amp; Wang (2019)</i>	GSE38240, GSE26910	14, 10	IGF2, GATA5, F10, CFI, AGTR1, <b>FOXA1</b> , BZRAP1-AS1, KRT8
<i>Tong, Song &amp; Deng (2019)</i>	GSE26910, GSE30174, GSE46602, GSE55945, GSE69223	140, 53	IKZF1, PPM1A, FBP1, SMCHD1, ALPL, CASP5, PYHIN1, DAPK1, CASP8
The present study	<b>GSE103512</b>	60, 7	KLK3, <b>CDH1</b> , KLK2, <b>FOXA1</b> , EPCAM

**Note:**

Bold fonts represent overlapped hub genes among studies.

*et al., 2009; Fan et al., 2018; Fang et al., 2017; He et al., 2018*) of which were based on a single GEO dataset whereas the other five studies (*Lu & Ding, 2019; Song et al., 2019b; Tan, Jin & Wang, 2019; Tong, Song & Deng, 2019; Zhao et al., 2017*) were integrated bioinformatic analyses based on multiple GEO datasets. The hub genes reported by the 10 eligible studies were extracted and compared with those identified in the present study. As marked in bold fonts in Table 6, there were some overlapped findings between our studies and other studies: our identified hub genes FOXA1, CDH1, and EPCAM were seen in two (*Endo et al., 2009; Tan, Jin & Wang, 2019*), one (*Fang et al., 2017*), and one (*Lu & Ding, 2019*) other studies, respectively.

Next, we further validated our findings using data from TCGA. GEPIA was applied to determine the expression differences of hub genes between PCa and NP tissues. As shown in Fig. 5A, mRNA levels of KLK3, CDH1, FOXA1, and EPCAM were significantly upregulated in PCa samples compared with NP samples; but there was no significant difference in the mRNA level of KLK2 between PCa and NP samples. Besides, we investigate the prognostic values of hub genes using TCGA data and conducted survival analyses with UCSC Xena online tools. As suggested in Fig. 5B, all five hub genes had no statistically significant impact on PCa patients' OSs. Furthermore, we put the top 10 significantly upregulated and downregulated DEGs into survival analysis and found two

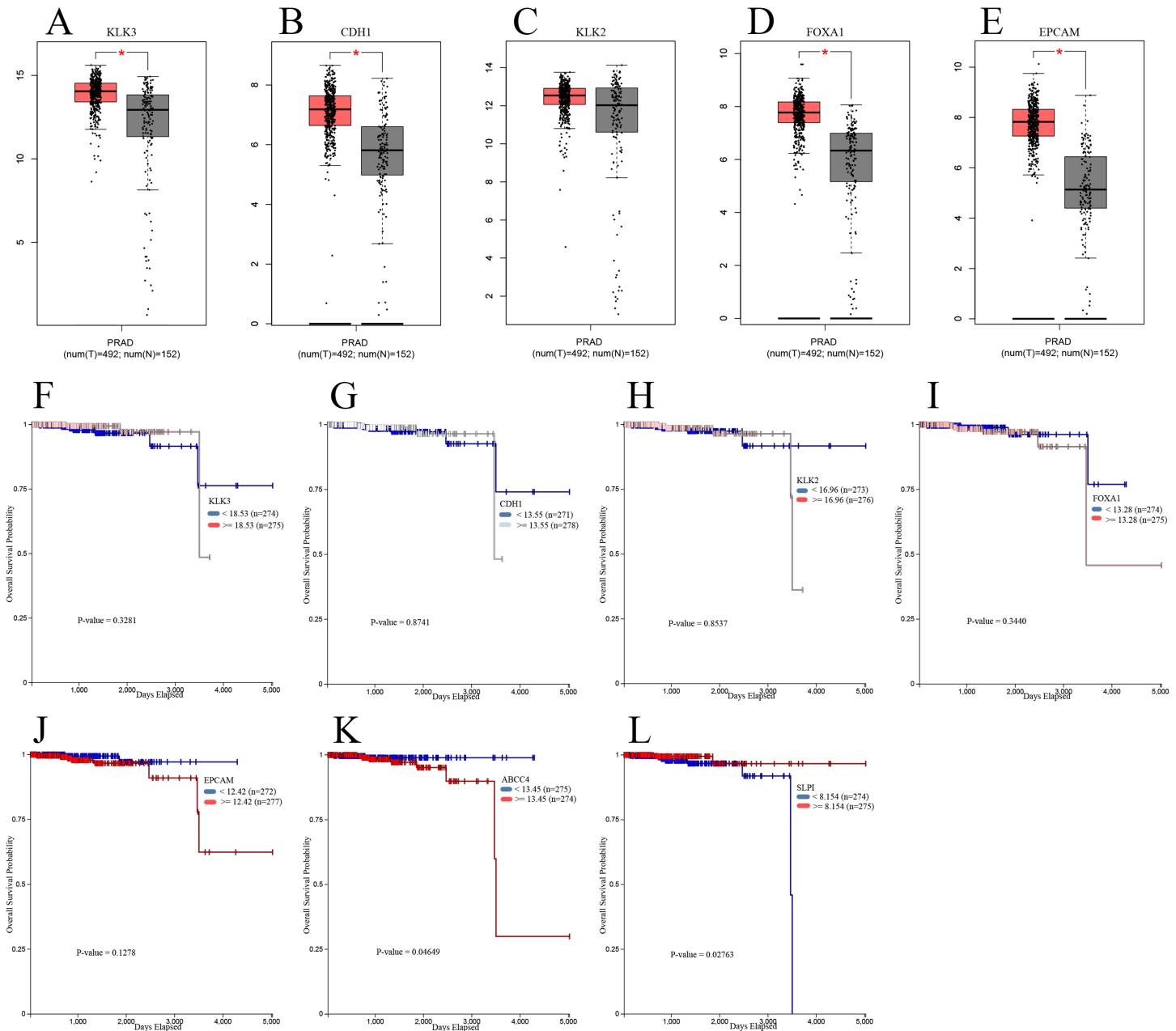
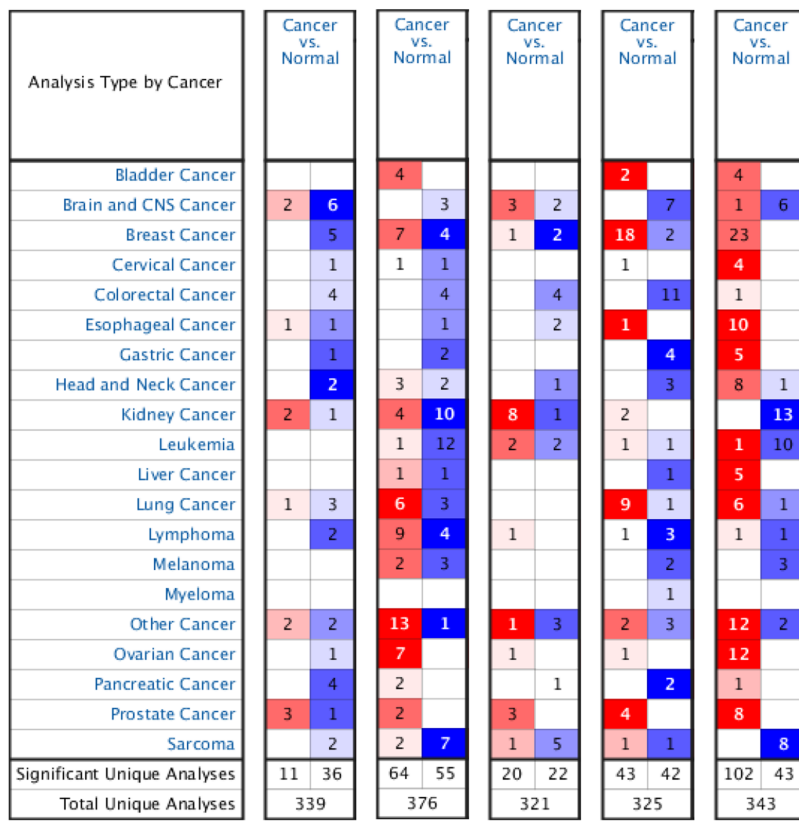


**Figure 5 Validation of hub genes using TCGA data.** Relative expression of hub genes between PCa and NP samples in the GEPPIA database (the threshold was set as  $|\log_2\text{FC}| = 1$ ,  $P = 0.05$ ,  $*P < 0.05$ ): (A) KLK3; (B) CDH1; (C) KLK2; (D) FOXA1; (E) EPCAM. The relationship of hub genes and top DEGs with the overall survival of TCGA PCa cohorts analyzed by the UCSC Xena online tools: (F) KLK3; (G) CDH1; (H) KLK2; (I) FOXA1; (J) EPCAM; (K) ABCC4; (L) SLPI. TCGA, The Cancer Genome Atlas; GEPPIA, the Gene Expression Profiling Interactive Analysis database; UCSC, University of California Santa Cruz.

Full-size DOI: 10.7717/peerj.7872/fig-5

genes had significant impact: the relative higher expression of ABCC4 (upregulated) as well as relative lower expression of SLPI (downregulated) were associated with poorer OS.

Furthermore, an overview of hub genes expression in multiple types of cancers revealed that all five hub genes were remarkably overexpressed in PCa tissues compared with NP tissues according to the Oncomine database (Fig. 6).



NOTE: An analysis may be counted in more than one cancer type.

**Figure 6** An overview of mRNA levels of hub genes in various types of cancer based on Oncomine data. The numbers in colored grids shows the counts of datasets with statistically significant mRNA overexpression (red) or low expression (blue) of genes. Grid color was determined by the best gene rank percentile for analysis within the grids. The threshold was set as gene rank percentile = All,  $P = 0.05$ , and FC = 2.

Full-size DOI: 10.7717/peerj.7872/fig-6

## DISCUSSION

As one of the leading healthcare concerns worldwide, PCa has become one of the most prevalent malignancies of adult males with an incidence of around 0.01% ([Jemal et al., 2010](#)). Although numerous progress has been made to uncover the molecular mechanisms of PCa development and progression, the outcomes remain obscure and the inconsistencies among different published studies are obvious ([Barbieri et al., 2017](#)). The main reason for such phenomenon is generally thought to be the complexity and heterogeneity nature of PCa as a whole ([Liu et al., 2019a](#); [Thomas & Pachynski, 2018](#)). Thus, it's of vital significance to perform further research in this regard to validate and update the information acquired.

In the current study, we first screened a total of 252 (186 upregulated and 66 downregulated) DEGs from the unused GEO dataset [GSE103512](#). The GO/KEGG pathway

enrichment analyses were implemented thereafter. Upregulated DEGs were mainly enriched in metabolic pathways, FA metabolism, and PPAR signaling pathway; whereas downregulated DEGs were mostly associated with protein digestion and absorption. Metabolism alteration is a hallmark of cancer. It is well demonstrated that the cancerous cellular metabolisms were urged to adapt themselves to the high proliferation rate and nutritional requirement so as to constantly support the increased cell division (Chandel, 2014; Sancho, Barneda & Heeschen, 2016). For PCa, one of the most noticeable metabolic changes is, as our results indicated, the FA or lipid metabolism (Deep & Schlaepfer, 2016; Yang et al., 2016). The lipid biosynthesis is essential for membrane formation and cell signaling; for instance, the metabolic intermediates of de novo lipogenesis can serve as second messengers and regulate PCa migration and invasion (Ferro et al., 2017). Moreover, the lipid metabolism of PCa is closely related to androgen by androgen receptor (AR) signaling. For examples, AR signaling can elevate the uptake of exogenous lipids by PCa cells (Liu, Zuckier & Ghesani, 2010) as well as stimulate adipose tissues to release FA (O'Reilly, House & Tomlinson, 2014). Furthermore, the PPARs family participate greatly in metabolic regulation. For example, PPAR $\gamma$  is a nuclear FA receptor which can interact with androgen receptor (AR) and regulate growth of PCa (Olokpa, Moss & Stewart, 2017). The FA-binding protein 5 (FABP5)-PPAR $\gamma$  signaling pathway promotes the malignant progression of castration-resistant PCa cells (Jing et al., 2000; Kawaguchi et al., 2016). Recently, the FABP5 inhibitor dmrFABP5 were illustrated to inhibit the FABP5-PPAR $\gamma$  pathway to suppress the malignant progression of PCa cells (Al-Jameel et al., 2019). Therefore, targeting the above pathways might aid in developing effective strategy for the treatment of PCa.

Next, we constructed PPI networks with the DEGs and identified the following top five hub genes: KLK3, CDH1, KLK2, FOXA1, and EPCAM. All hub genes exhibited upregulated expressions in PCa compared to NP tissues. Both KLK3 and KLK2 belong to the Kallikrein-related peptidases (KLKs) family. Expressed and secreted by glandular epithelia of many organs including skin, mammary gland, prostate, colon, pancreas and brain, KLKs are a sort of serine proteases existed in the body fluids excreted by the above organs such as sweat, milk, and seminal fluid, involving in various physiological functions like electrolyte balance, extracellular matrix remodeling, and prohormone processing (Borgono, Michael & Diamandis, 2004; Shaw & Diamandis, 2007). Aberrant expression of KLKs can be found in several kinds of malignancies including ovarian cancer (Loessner et al., 2018), breast cancer (Figueroa et al., 2018), gastrointestinal cancer (Kontos et al., 2013), and PCa (Mavridis, Avgeris & Scorilas, 2014; McDonald & Parsons, 2016). Further on, it was suggested that KLKs could lead to proliferation of the epithelium via protease-activated receptors, which might contribute to PCa development (Ramsay et al., 2008). Several studies have highlighted the association between KLK3 gene polymorphism and susceptibility to PCa (Chen & Xin, 2017; Ding et al., 2018; Motamed et al., 2019), and Zambon et al. (2012) successfully combined the KLK3 genetics analysis and free-to-total PSA ratio for PCa diagnosis. Similarly, KLK2 was reported to be potential marker for diagnosis because its polymorphism can increase vulnerability to PCa (David et al., 2002; Nam et al., 2006). And more notably, the loss of miR-378

(a regulator of KLK2) in PCa was found to be correlated with aggressive phenotype and short-term relapse events ([Avgeris, Stravodimos & Scorilas, 2014](#)). Both KLK2 and KLK3 were reported to elevate the level of insulin-like growth factor (IGF) by cleaving the IGF-binding proteins, which consequently affects cell survival, mitogenesis, and differentiation. Analogously, KLK3 can cleave the TGF $\beta$ -binding proteins and activate TGF $\beta$ , resulting in cell proliferation ([Borgono, Michael & Diamandis, 2004](#)).

The encoding product of CDH1 gene, namely E-cadherin, participates in cell-cell adhesion and the maintenance of cell differentiation as well as normal structure of epithelium ([Mayer et al., 1993; Takeichi, 1995](#)). Pathologically, inactivation or absence of CDH1 expression can decrease intercellular junctions and thus promote cancer invasion and metastasis, as seen in diffuse gastric cancer ([Melo et al., 2017](#)) and lobular breast cancer ([McVeigh et al., 2014](#)). Contrary to expectation, our results indicated that CDH1 expression turned out to be significantly upregulated in PCa compared to NP tissues. Consistent with our results, another study using the [GSE26910](#) dataset also found overexpressed CDH1 in PCa samples ([Fang et al., 2017](#)). It was hypothesized that overexpression of CDH1 might have an impact on oncogenesis since previous research has indicated the intercellular adhesion between cancer and normal cells were enhanced in the late stage of tumor formation ([Albelda, 1993](#)). Plus, polymorphism of CDH1 was also found to elevate the risk of PCa ([Imtiaz et al., 2019; Qiu et al., 2009](#)). Future work is merited to explore the expression changes of CDH1 in different stages of PCa.

Forkhead Box A1, also known as hepatocyte nuclear factor 3 $\alpha$ , is a transcription factor that plays important roles in development as well as cancer formation ([Bernardo & Keri, 2012](#)). FOXA1 has multiple impact on PCa, including (1) controls the morphogenesis and cell differentiation of prostate ([Gao et al., 2005](#)); (2) facilitates AR transactivation which is essential for PCa proliferation and survival ([Zhao, Tindall & Huang, 2014](#)); (3) inhibits PCa progress towards neuroendocrine prostate cancer, whose prognosis is worse ([Kim et al., 2017](#)); (4) downregulates TGF- $\beta$  signaling and thus suppresses castration-resistant prostate cancer progression ([Song et al., 2019a](#)). Our findings were validated by another expression profiling study ([Endo et al., 2009](#)), and the complexity of functions of FOXA1 still calls for further research to fully interpret its role in PCa development and progression.

Epithelial cell adhesion molecule encodes epithelial cell adhesion molecule, also known as CD326, is usually high expressed in cancer tissues and participates in intercellular adhesion limitation, cell signaling, migration, proliferation, and differentiation ([Maetzel et al., 2009](#)). Consistent with our results, EPCAM is shown to be overexpressed in localized and metastatic PCa ([Massoner et al., 2014](#)). Other integrated bioinformatic analysis using four GEO datasets also validated our findings ([Lu & Ding, 2019](#)).

When it comes to validation of the identified hub genes, three of them (CDH1, FOXA1, and EPCAM) were validated by other studies using relevant GEO datasets; four genes (except KLK2) were validated by TCGA data; and all five genes were validated by the Oncomine data. This implied their potentials as effective and reliable biomarkers for diagnosis and as possible therapeutic targets. However, in survival analysis using TCGA cohorts, all hub genes turned out to have insignificant impact on PCa patients' OS. To add

readability, we put the top 10 upregulated and downregulated DEGs into the survival analysis, outputting two significant genes, namely ABCC4 and SLPI. ABCC4 (ATP-cassette binding protein 4), which was significantly upregulated as our results revealed, its relatively higher expression was associated with poorer OS of PCa patients. This negative effect of ABCC4 expression toward PCa might result from that ABCC4 could decrease the efficacy of docetaxel in treating PCa cells (*Oprea-Lager et al., 2013*). Conversely, the relatively higher level of downregulated DEG SLPI (Stomatin-like protein 1) was related to better OS of PCa patients. There are not many studies focused on SLPI. Intriguingly, it is revealed that overexpression of SLPI stabilizes F-box protein Fbw7- $\gamma$  by inhibiting its degradation, which is implicated in the degradation of oncogene c-Myc (*Zhang, MacDonald & Koepp, 2012*). So SLPI might impact negatively on cell proliferation of PCa through the above mechanism. Therefore, these two genes might hopefully serve as prognostic indicators for PCa patients.

We also conducted a module analysis on the existing PPI network and selected the top two significant modules for the ensuing KEGG pathway enrichment analysis of the genes contained. The results demonstrated that the genes in Module 1 are mainly enriched in adherens junction and Hippo signaling pathway; while the genes in Module 2 are mainly enriched in FA metabolism, fatty acid biosynthesis, PPAR signaling pathway, and FA degradation. Apparently, the modules KEGG analyses were quite conformed to the overall KEGG results. The FA metabolism related pathways, PPAR signaling pathway, and cell adhesion-related hub genes and pathways were already discussed above. It was demonstrated that the activation of Hippo signaling pathway regulates cell growth and proliferation by inhibiting YAP and TAZ transcription co-activators, and its dysregulation impacts significantly on development of cancers including colon, liver, breast, lung, ovary, and prostate (*Salem & Hansen, 2019; Yu, Zhao & Guan, 2015*).

## CONCLUSIONS

By bioinformatic analyses including GO/KEGG enrichment, PPI network, hub gene identification, and module analysis, the current study validated KLK3, CDHI, FOXA1, and EPCAM might potentially serve as effective and reliable molecular biomarkers for diagnosis of PCa; and ABCC4 and SLPI might be utilized as prognostic indicators of PCa. However, further basic and clinical researches are necessary for the verification of the clinical value of our findings.

## ACKNOWLEDGEMENTS

Special thanks to Mr. Fucai Tang for his assistance in the use of R programming Language.

## ADDITIONAL INFORMATION AND DECLARATIONS

### Funding

This work was supported by the Guangdong Provincial Science and Technology Plan Project (No. 2017B030314108). The funders had no role in study design, data collection and analysis, decision to publish, or preparation of the manuscript.

## Grant Disclosures

The following grant information was disclosed by the authors:

Guangdong Provincial Science and Technology Plan: 2017B030314108.

## Competing Interests

The authors declare that they have no competing interests.

## Author Contributions

- Zihao He conceived and designed the experiments, performed the experiments, analyzed the data, prepared figures and/or tables, authored or reviewed drafts of the paper, approved the final draft.
- Xiaolu Duan conceived and designed the experiments, contributed reagents/materials/analysis tools, authored or reviewed drafts of the paper, approved the final draft.
- Guohua Zeng conceived and designed the experiments, contributed reagents/materials/analysis tools, authored or reviewed drafts of the paper, approved the final draft.

## Data Availability

The following information was supplied regarding data availability:

Data is available at NCBI GEO: [GSE103512](#).

## Supplemental Information

Supplemental information for this article can be found online at <http://dx.doi.org/10.7717/peerj.7872#supplemental-information>.

## REFERENCES

- Al-Jameel W, Gou X, Jin X, Zhang J, Wei Q, Ai J, Li H, Al-Bayati A, Platt-Higgins A, Pettitt A, Rudland PS, Ke Y. 2019. Inactivated FABP5 suppresses malignant progression of prostate cancer cells by inhibiting the activation of nuclear fatty acid receptor PPAR $\gamma$ . *Genes Cancer* 10(3–4):80–96 DOI [10.18632/genescancer.192](https://doi.org/10.18632/genescancer.192).
- Albelda SM. 1993. Role of integrins and other cell adhesion molecules in tumor progression and metastasis. *Laboratory Investigation* 68(1):4–17.
- Avgeris M, Stravodimos K, Scorilas A. 2014. Loss of miR-378 in prostate cancer, a common regulator of KLK2 and KLK4, correlates with aggressive disease phenotype and predicts the short-term relapse of the patients. *Biological Chemistry* 395(9):1095–1104 DOI [10.1515/hsz-2014-0150](https://doi.org/10.1515/hsz-2014-0150).
- Bandettini WP, Kellman P, Mancini C, Booker OJ, Vasu S, Leung SW, Wilson JR, Shanbhag SM, Chen MY, Arai AE. 2012. MultiContrast delayed enhancement (MCODE) improves detection of subendocardial myocardial infarction by late gadolinium enhancement cardiovascular magnetic resonance: a clinical validation study. *Journal of Cardiovascular Magnetic Resonance* 14(1):83 DOI [10.1186/1532-429X-14-83](https://doi.org/10.1186/1532-429X-14-83).
- Barbieri CE, Chinnaiyan AM, Lerner SP, Swanton C, Rubin MA. 2017. The emergence of precision urologic oncology: a collaborative review on biomarker-driven therapeutics. *European Urology* 71(2):237–246 DOI [10.1016/j.eururo.2016.08.024](https://doi.org/10.1016/j.eururo.2016.08.024).
- Bernardo GM, Keri RA. 2012. FOXA1: a transcription factor with parallel functions in development and cancer. *Bioscience Reports* 32(2):113–130 DOI [10.1042/BSR20110046](https://doi.org/10.1042/BSR20110046).

- Borgono CA, Michael IP, Diamandis EP.** 2004. Human tissue kallikreins: physiologic roles and applications in cancer. *Molecular Cancer Research* 2(5):257–280.
- Brouwer-Visser J, Cheng WY, Bauer-Mehren A, Maisel D, Lechner K, Andersson E, Dudley JT, Milletti F.** 2018. Regulatory T-cell genes drive altered immune microenvironment in adult solid cancers and allow for immune contextual patient subtyping. *Cancer Epidemiology Biomarkers & Prevention* 27(1):103–112 DOI 10.1158/1055-9965.EPI-17-0461.
- Chandel NS.** 2014. Mitochondria as signaling organelles. *BMC Biology* 12:34 DOI 10.1186/1741-7007-12-34.
- Chen JH, He HC, Jiang FN, Militar J, Ran PY, Qin GQ, Cai C, Chen XB, Zhao J, Mo ZY, Chen YR, Zhu JG, Liu X, Zhong WD.** 2012. Analysis of the specific pathways and networks of prostate cancer for gene expression profiles in the Chinese population. *Medical Oncology* 29(3):1972–1984 DOI 10.1007/s12032-011-0088-5.
- Chen C, Xin Z.** 2017. Single-nucleotide polymorphism rs1058205 of KLK3 is associated with the risk of prostate cancer: a case-control study of Han Chinese men in Northeast China. *Medicine* 96(10):e6280 DOI 10.1097/MD.00000000000006280.
- Clough E, Barrett T.** 2016. The gene expression omnibus database. *Methods in Molecular Biology* 1418(5235):93–110 DOI 10.1007/978-1-4939-3578-9\_5.
- David A, Mabjeesh N, Azar I, Biton S, Engel S, Bernstein J, Romano J, Avidor Y, Waks T, Eshhar Z, Langer SZ, Lifschitz-Mercer B, Matzkin H, Rotman G, Toporik A, Savitsky K, Mintz L.** 2002. Unusual alternative splicing within the human kallikrein genes KLK2 and KLK3 gives rise to novel prostate-specific proteins. *Journal of Biological Chemistry* 277(20):18084–18090 DOI 10.1074/jbc.M102285200.
- Deep G, Schlaepfer IR.** 2016. Aberrant lipid metabolism promotes prostate cancer: role in cell survival under Hypoxia and Extracellular vesicles biogenesis. *International Journal of Molecular Sciences* 17(7):1061 DOI 10.3390/ijms17071061.
- Dennis G Jr, Sherman BT, Hosack DA, Yang J, Gao W, Lane HC, Lempicki RA.** 2003. DAVID: database for annotation, visualization, and integrated discovery. *Genome Biology* 4(5):P3 DOI 10.1186/gb-2003-4-5-p3.
- Ding W-H, Ren K-W, Yue C, Zou J-G, Zuo L, Zhang L-F, Bai Y, Okada A, Yasui T, Mi Y-Y.** 2018. Association between three genetic variants in kallikrein 3 and prostate cancer risk. *Bioscience Reports* 38(6):BSR20181151 DOI 10.1042/bsr20181151.
- Endo T, Uzawa K, Suzuki H, Tanzawa H, Ichikawa T.** 2009. Characteristic gene expression profiles of benign prostatic hypertrophy and prostate cancer. *International Journal of Oncology* 35(5):499–509 DOI 10.3892/ijo\_00000361.
- Fan S, Liang Z, Gao Z, Pan Z, Han S, Liu X, Zhao C, Yang W, Pan Z, Feng W.** 2018. Identification of the key genes and pathways in prostate cancer. *Oncology Letters* 16(5):6663–6669 DOI 10.3892/ol.2018.9491.
- Fang E, Zhang X, Wang Q, Wang D.** 2017. Identification of prostate cancer hub genes and therapeutic agents using bioinformatics approach. *Cancer Biomarkers* 20(4):553–561 DOI 10.3233/CBM-170362.
- Ferro M, Terracciano D, Buonerba C, Lucarelli G, Bottero D, Perdona S, Autorino R, Serino A, Cantiello F, Damiano R, Andras I, De Placido S, Di Lorenzo G, Battaglia M, Jereczek-Fossa BA, Mirone V, De Cobelli O.** 2017. The emerging role of obesity, diet and lipid metabolism in prostate cancer. *Future Oncology* 13(3):285–293 DOI 10.2217/fon-2016-0217.
- Figueroa CD, Molina L, Bhoola KD, Ehrenfeld P.** 2018. Overview of tissue kallikrein and kallikrein-related peptidases in breast cancer. *Biological Chemistry* 399(9):937–957 DOI 10.1515/hsz-2018-0111.

- Gandaglia G, Albers P, Abrahamsson PA, Briganti A, Catto JWF, Chapple CR, Montorsi F, Mottet N, Roobol MJ, Sonksen J, Wirth M, Van Poppel H.** 2019. Structured population-based prostate-specific antigen screening for prostate cancer: the European Association of Urology Position in 2019. *European Urology* **76**(2):142–150 DOI [10.1016/j.eururo.2019.04.033](https://doi.org/10.1016/j.eururo.2019.04.033).
- Gao N, Ishii K, Mirosevich J, Kuwajima S, Oppenheimer SR, Roberts RL, Jiang M, Yu X, Shappell SB, Caprioli RM, Stoffel M, Hayward SW, Matusik RJ.** 2005. Forkhead box A1 regulates prostate ductal morphogenesis and promotes epithelial cell maturation. *Development* **132**(15):3431–3443 DOI [10.1242/dev.01917](https://doi.org/10.1242/dev.01917).
- He Z, Tang F, Lu Z, Huang Y, Lei H, Li Z, Zeng G.** 2018. Analysis of differentially expressed genes, clinical value and biological pathways in prostate cancer. *American Journal of Translational Research* **10**(5):1444–1456.
- Imtiaz H, Afroz S, Hossain MA, Bellah SF, Rahman MM, Kadir MS, Sultana R, Mazid MA, Rahman MM.** 2019. Genetic polymorphisms in *CDH1* and *Exo1* genes elevate the prostate cancer risk in Bangladeshi population. *Tumor Biology* **41**(3):1010428319830837 DOI [10.1177/1010428319830837](https://doi.org/10.1177/1010428319830837).
- Inahara M, Suzuki H, Kojima S, Komiya A, Fukasawa S, Imamoto T, Naya Y, Ichikawa T.** 2006. Improved prostate cancer detection using systematic 14-core biopsy for large prostate glands with normal digital rectal examination findings. *Urology* **68**(4):815–819 DOI [10.1016/j.urology.2006.05.010](https://doi.org/10.1016/j.urology.2006.05.010).
- Jemal A, Siegel R, Xu J, Ward E.** 2010. Cancer Statistics, 2010. *CA: A Cancer Journal for Clinicians* **60**(5):277–300 DOI [10.3322/caac.20073](https://doi.org/10.3322/caac.20073).
- Jing C, Beesley C, Foster CS, Rudland PS, Fujii H, Ono T, Chen H, Smith PH, Ke Y.** 2000. Identification of the messenger RNA for human cutaneous fatty acid-binding protein as a metastasis inducer. *Cancer Research* **60**:2390–2398.
- Kawaguchi K, Kinameri A, Suzuki S, Senga S, Ke Y, Fujii H.** 2016. The cancer-promoting gene fatty acid-binding protein 5 (FABP5) is epigenetically regulated during human prostate carcinogenesis. *Biochemical Journal* **473**(4):449–461 DOI [10.1042/BJ20150926](https://doi.org/10.1042/BJ20150926).
- Kim J, Jin H, Zhao JC, Yang YA, Li Y, Yang X, Dong X, Yu J.** 2017. FOXA1 inhibits prostate cancer neuroendocrine differentiation. *Oncogene* **36**(28):4072–4080 DOI [10.1038/onc.2017.50](https://doi.org/10.1038/onc.2017.50).
- Kontos CK, Mavridis K, Talieri M, Scorilas A.** 2013. Kallikrein-related peptidases (KLKs) in gastrointestinal cancer: mechanistic and clinical aspects. *Thrombosis and Haemostasis* **110**(09):450–457 DOI [10.1160/TH12-11-0791](https://doi.org/10.1160/TH12-11-0791).
- Liu J, Near A, Chiarappa JA, Wada K, Tse J, Burudpakdee C, Behl A, Ranganath R, Antonarakis ES.** 2019a. Clinical outcomes associated with pathogenic genomic instability mutations in prostate cancer: a retrospective analysis of US pharmacy and medical claims data. *Journal of Medical Economics* **22**(10):1080–1087 DOI [10.1080/13696998.2019.1649267](https://doi.org/10.1080/13696998.2019.1649267).
- Liu J, Wang Z-Q, Li M, Zhou M-Y, Yu Y-F, Zhan W-W.** 2019b. Establishment of two new predictive models for prostate cancer to determine whether to require prostate biopsy when the PSA level is in the diagnostic gray zone (4–10 ng ml<sup>-1</sup>). *Asian Journal of Andrology* **21**:1–4 DOI [10.4103/aja.aja\\_46\\_19](https://doi.org/10.4103/aja.aja_46_19).
- Liu Y, Zuckier LS, Ghesani NV.** 2010. Dominant uptake of fatty acid over glucose by prostate cells: a potential new diagnostic and therapeutic approach. *Anticancer Research* **30**:369–374.
- Loessner D, Goettig P, Preis S, Felber J, Bronger H, Clements JA, Dorn J, Magdolen V.** 2018. Kallikrein-related peptidases represent attractive therapeutic targets for ovarian cancer. *Expert Opinion on Therapeutic Targets* **22**(9):745–763 DOI [10.1080/14728222.2018.1512587](https://doi.org/10.1080/14728222.2018.1512587).
- Lu W, Ding Z.** 2019. Identification of key genes in prostate cancer gene expression profile by bioinformatics. *Cancer Cell International* **51**(1):e13169 DOI [10.1111/and.13169](https://doi.org/10.1111/and.13169).

- Maetzel D, Denzel S, Mack B, Canis M, Went P, Benk M, Kieu C, Papior P, Baeuerle PA, Munz M, Gires O.** 2009. Nuclear signalling by tumour-associated antigen EpCAM. *Nature Cell Biology* 11(2):162–171 DOI [10.1038/ncb1824](https://doi.org/10.1038/ncb1824).
- Massoner P, Thomm T, Mack B, Untergasser G, Martowicz A, Bobowski K, Klocker H, Gires O, Puhr M.** 2014. EpCAM is overexpressed in local and metastatic prostate cancer, suppressed by chemotherapy and modulated by MET-associated miRNA-200c/205. *British Journal of Cancer* 111(5):955–964 DOI [10.1038/bjc.2014.366](https://doi.org/10.1038/bjc.2014.366).
- Mavridis K, Avgeris M, Scorilas A.** 2014. Targeting kallikrein-related peptidases in prostate cancer. *Expert Opinion on Therapeutic Targets* 18(4):365–383 DOI [10.1517/14728222.2014.880693](https://doi.org/10.1517/14728222.2014.880693).
- Mayer B, Johnson JP, Leitl F, Jauch KW, Heiss MM, Schildberg FW, Birchmeier W, Funke I.** 1993. E-cadherin expression in primary and metastatic gastric cancer: down-regulation correlates with cellular dedifferentiation and glandular disintegration. *Cancer Research* 53(7):1690–1695.
- McDonald ML, Parsons JK.** 2016. 4-Kallikrein test and Kallikrein markers in prostate cancer screening. *Urologic Clinics of North America* 43(1):39–46 DOI [10.1016/j.ucl.2015.08.004](https://doi.org/10.1016/j.ucl.2015.08.004).
- McVeigh TP, Choi JK, Miller NM, Green AJ, Kerin MJ.** 2014. Lobular breast cancer in a CDH1 splice site mutation carrier: case report and review of the literature. *Clinical Breast Cancer* 14(2):e47–e51 DOI [10.1016/j.clbc.2013.10.007](https://doi.org/10.1016/j.clbc.2013.10.007).
- Melo S, Figueiredo J, Fernandes MS, Goncalves M, Morais-de-Sa E, Sanches JM, Seruca R.** 2017. Predicting the functional impact of CDH1 missense mutations in hereditary diffuse gastric cancer. *International Journal of Molecular Sciences* 18(12):2687 DOI [10.3390/ijms18122687](https://doi.org/10.3390/ijms18122687).
- Motamedi RK, Sarhangi N, Afshari M, Sattari M, Jamaldini SH, Samzadeh M, Mohsen Ziae SA, Pourmand GR, Hasanzad M.** 2019. Kallikrein-related peptidase 3 common genetic variant and the risk of prostate cancer. *Journal of Cellular Biochemistry* 120(9):14822–14830 DOI [10.1002/jcb.28743](https://doi.org/10.1002/jcb.28743).
- Nam RK, Zhang WW, Klotz LH, Trachtenberg J, Jewett MA, Sweet J, Toi A, Teahan S, Venkateswaran V, Sugar L, Loblaw A, Siminovitch K, Narod SA.** 2006. Variants of the hK2 protein gene (KLK2) are associated with serum hK2 levels and predict the presence of prostate cancer at biopsy. *Clinical Cancer Research* 12(21):6452–6458 DOI [10.1158/1078-0432.CCR-06-1485](https://doi.org/10.1158/1078-0432.CCR-06-1485).
- O'Reilly MW, House PJ, Tomlinson JW.** 2014. Understanding androgen action in adipose tissue. *Journal of Steroid Biochemistry and Molecular Biology* 143:277–284 DOI [10.1016/j.jsbmb.2014.04.008](https://doi.org/10.1016/j.jsbmb.2014.04.008).
- Olokpa E, Moss PE, Stewart LV.** 2017. Crosstalk between the androgen receptor and PPAR gamma signaling pathways in the prostate. *PPAR Research* 2017(2):9456020 DOI [10.1155/2017/9456020](https://doi.org/10.1155/2017/9456020).
- Oprea-Lager DE, Bijnsdorp IV, Van Moorselaar RJ, Van Den Eertwegh AJ, Hoekstra OS, Geldof AA.** 2013. ABCC4 decreases docetaxel and not cabazitaxel efficacy in prostate cancer cells in vitro. *Anticancer Research* 33(2):387–391.
- Qiu L-X, Li R-T, Zhang J-B, Zhong W-Z, Bai J-L, Liu B-R, Zheng M-H, Qian X-P.** 2009. The E-cadherin (CDH1)-160 C/A polymorphism and prostate cancer risk: a meta-analysis. *European Journal of Human Genetics* 17(2):244–249 DOI [10.1038/ejhg.2008.157](https://doi.org/10.1038/ejhg.2008.157).
- Ramsay AJ, Reid JC, Adams MN, Samaratunga H, Dong Y, Clements JA, Hooper JD.** 2008. Prostatic trypsin-like kallikrein-related peptidases (KLKs) and other prostate-expressed tryptic proteinases as regulators of signalling via proteinase-activated receptors (PARs). *Biological Chemistry* 389(6):653–668 DOI [10.1515/BC.2008.078](https://doi.org/10.1515/BC.2008.078).

- Rhodes DR, Yu J, Shanker K, Deshpande N, Varambally R, Ghosh D, Barrette T, Pandey A, Chinnaiyan AM.** 2004. ONCOMINE: a cancer microarray database and integrated data-mining platform. *Neoplasia* **6**(1):1–6 DOI [10.1016/S1476-5586\(04\)80047-2](https://doi.org/10.1016/S1476-5586(04)80047-2).
- Ritchie ME, Phipson B, Wu D, Hu Y, Law CW, Shi W, Smyth GK.** 2015. limma powers differential expression analyses for RNA-sequencing and microarray studies. *Nucleic Acids Research* **43**(7):e47–e47 DOI [10.1093/nar/gkv007](https://doi.org/10.1093/nar/gkv007).
- Salem O, Hansen CG.** 2019. The hippo pathway in prostate cancer. *Cells* **8**(4):370 DOI [10.3390/cells8040370](https://doi.org/10.3390/cells8040370).
- Sancho P, Barneda D, Heeschen C.** 2016. Hallmarks of cancer stem cell metabolism. *British Journal of Cancer* **114**(12):1305–1312 DOI [10.1038/bjc.2016.152](https://doi.org/10.1038/bjc.2016.152).
- Shaw JLV, Diamandis EP.** 2007. Distribution of 15 human kallikreins in tissues and biological fluids. *Clinical Chemistry* **53**(8):1423–1432 DOI [10.1373/clinchem.2007.088104](https://doi.org/10.1373/clinchem.2007.088104).
- Siegel RL, Miller KD, Jemal A.** 2019. Cancer statistics, 2019. *CA: A Cancer Journal for Clinicians* **69**(1):7–34 DOI [10.3322/caac.21551](https://doi.org/10.3322/caac.21551).
- Song B, Park SH, Zhao JC, Fong KW, Li S, Lee Y, Yang YA, Sridhar S, Lu X, Abdulkadir SA, Vessella RL, Morrissey C, Kuzel TM, Catalona W, Yang X, Yu J.** 2019a. Targeting FOXA1-mediated repression of TGF-beta signaling suppresses castration-resistant prostate cancer progression. *Journal of Clinical Investigation* **129**(2):569–582 DOI [10.1172/JCI122367](https://doi.org/10.1172/JCI122367).
- Song ZY, Chao F, Zhuo Z, Ma Z, Li W, Chen G.** 2019b. Identification of hub genes in prostate cancer using robust rank aggregation and weighted gene co-expression network analysis. *Aging* **11**:4736–4756 DOI [10.18632/aging.102087](https://doi.org/10.18632/aging.102087).
- Stelzl U, Worm U, Lalowski M, Haenig C, Brembeck FH, Goehler H, Stroedicke M, Zenkner M, Schoenherr A, Koeppen S, Timm J, Mintzlaff S, Abraham C, Bock N, Kietzmann S, Goedde A, Toksoz E, Droege A, Krobisch S, Korn B, Birchmeier W, Lehrach H, Wanker EE.** 2005. A human protein-protein interaction network: a resource for annotating the proteome. *Cell* **122**(6):957–968 DOI [10.1016/j.cell.2005.08.029](https://doi.org/10.1016/j.cell.2005.08.029).
- Takeichi M.** 1995. Morphogenetic roles of classic cadherins. *Current Opinion in Cell Biology* **7**(5):619–627 DOI [10.1016/0955-0674\(95\)80102-2](https://doi.org/10.1016/0955-0674(95)80102-2).
- Tan J, Jin X, Wang K.** 2019. Integrated bioinformatics analysis of potential biomarkers for prostate cancer. *Pathology & Oncology Research* **25**(2):455–460 DOI [10.1007/s12253-017-0346-8](https://doi.org/10.1007/s12253-017-0346-8).
- Tang Z, Li C, Kang B, Gao G, Li C, Zhang Z.** 2017. GEPIA: a web server for cancer and normal gene expression profiling and interactive analyses. *Nucleic Acids Research* **45**(W1):W98–W102 DOI [10.1093/nar/gkx247](https://doi.org/10.1093/nar/gkx247).
- Thomas TS, Pachynski RK.** 2018. Treatment of advanced prostate cancer. *Missouri Medicine* **115**:156–161.
- Tong Y, Song Y, Deng S.** 2019. Combined analysis and validation for DNA methylation and gene expression profiles associated with prostate cancer. *Cancer Cell International* **19**:50 DOI [10.1186/s12935-019-0753-x](https://doi.org/10.1186/s12935-019-0753-x).
- Von Mering C, Huynen M, Jaeggi D, Schmidt S, Bork P, Snel B.** 2003. STRING: a database of predicted functional associations between proteins. *Nucleic Acids Research* **31**(1):258–261 DOI [10.1093/nar/gkg034](https://doi.org/10.1093/nar/gkg034).
- Yang M, Ayuningtyas A, Kenfield SA, Sesso HD, Campos H, Ma J, Stampfer MJ, Chavarro JE.** 2016. Blood fatty acid patterns are associated with prostate cancer risk in a prospective nested case-control study. *Cancer Causes & Control* **27**(9):1153–1161 DOI [10.1007/s10552-016-0794-6](https://doi.org/10.1007/s10552-016-0794-6).
- Yu F-X, Zhao B, Guan K-L.** 2015. Hippo pathway in organ size control, tissue homeostasis, and cancer. *Cell* **163**(4):811–828 DOI [10.1016/j.cell.2015.10.044](https://doi.org/10.1016/j.cell.2015.10.044).

- Zambon C-F, Prayer-Galetti T, Basso D, Padoan A, Rossi E, Secco S, Peloso M, Fogar P, Navaglia F, Moz S, Zattoni F, Plebani M.** 2012. Effectiveness of the combined evaluation of KLK3 genetics and free-to-total prostate specific antigen ratio for prostate cancer diagnosis. *Journal of Urology* **188**(4):1124–1130 DOI [10.1016/j.juro.2012.06.030](https://doi.org/10.1016/j.juro.2012.06.030).
- Zhang W, MacDonald EM, Koepp DM.** 2012. The stomatin-like protein SLP-1 and Cdk2 interact with the F-Box protein Fbw7-gamma. *PLOS ONE* **7**(10):e47736 DOI [10.1371/journal.pone.0047736](https://doi.org/10.1371/journal.pone.0047736).
- Zhao Y, Tindall DJ, Huang H.** 2014. Modulation of androgen receptor by FOXA1 and FOXO1 factors in prostate cancer. *International Journal of Biological Sciences* **10**(6):614–619 DOI [10.7150/ijbs.8389](https://doi.org/10.7150/ijbs.8389).
- Zhao R, Wang Y, Zhang M, Gu X, Wang W, Tan J, Wei X, Jin N.** 2017. Screening of potential therapy targets for prostate cancer using integrated analysis of two gene expression profiles. *Oncology Letters* **14**:5361–5369 DOI [10.3892/ol.2017.6879](https://doi.org/10.3892/ol.2017.6879).